1 The nature of windstorms and wind-induced damage

1.1 Introduction

Wind loading competes with seismic loading as the dominant environmental loading for structures. They have produced roughly equal amounts of damage over a long time period, although large damaging earthquakes have tended to occur less often than severe windstorms. On almost every day of the year a severe windstorm is happening somewhere on earth – although many storms are small and localized. In the tropical oceans, the most severe of all wind events – tropical cyclones – are generated. When these storms make landfall on populated coastlines, their effects can be devastating.

In this introductory chapter, the meteorology of severe wind storms – *gales* produced by large extra-tropical depressions, *tropical cyclones*, and *downbursts*, squall lines and *tornados* associated with thunderstorms, is explained, including the expected horizontal variation in wind speed during these events. The history of damaging wind events, particularly those of the last twenty-five years, is discussed, focussing on the lessons learnt from them by the structural engineering profession. The behaviour of flying debris, a major source of damage in severe windstorms, is outlined. Insurance aspects are discussed, including the recent development of loss models, based on historical data on the occurrences of large severe storms, the spatial characteristics for the wind speeds within them, and assumed relationships between building damage and wind speed.

1.2 Meteorological aspects

Wind is air movement relative to the earth, driven by several different forces, especially pressure differences in the atmosphere, which are themselves produced by differential solar heating of different parts of the earth's surface, and forces generated by the rotation of the earth. The differences in solar radiation between the poles and the equator, produce temperature and pressure differences. These, together with the effects of the earth's rotation set up large-scale circulation systems in the atmosphere, with both horizontal and vertical orientations. The result of these circulations is that the prevailing wind directions in the tropics, and near the poles, tend to be easterly. Westerly winds dominate in the temperate latitudes.

Local severe winds may also originate from local convective effects (*thunderstorms*), or from the uplift of air masses produced by mountain ranges (*downslope winds*). Severe tropical cyclones, known in some parts of the world as *hurricanes* and as *typhoons*, generate extremely strong winds over some parts of the tropical oceans and coastal regions, in latitudes from 10 to about 30 degrees, both north and south of the equator.

For all types of severe storms, the wind is highly turbulent or gusty. The turbulence or gustiness is produced by eddies or vortices within the air flow which are generated by frictional interaction at ground level, or by shearing action between air moving in opposite

directions at altitude. These processes are illustrated in Figure 1.1 for downdrafts generated by thunderstorms, and for larger storms such as gales or tropical cyclones which are of the 'boundary-layer' type.

1.2.1 Pressure gradient

The two most important forces acting on the upper level air in the 'free atmosphere', that is above the frictional effects of the earth's boundary layer, are: the pressure gradient force and the Coriolis force.

It is shown in elementary texts on fluid mechanics that, at a point in a fluid in which there is a pressure gradient, $\partial p/\partial x$, in a given direction, x, in a Cartesian coordinate system, there is a resulting force per unit mass given by equation (1.1)

Pressure gradient force per unit mass

$$= -\left(\frac{1}{\rho_a}\right)\frac{\partial p}{\partial x} \tag{1.1}$$

where ρ_a is the density of air.

This force acts from a high pressure region to a low pressure region.

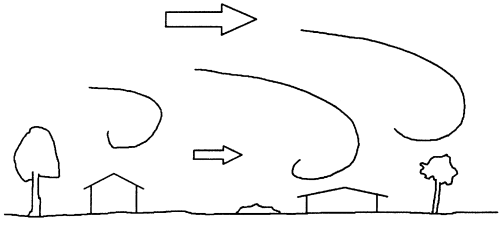

(a)

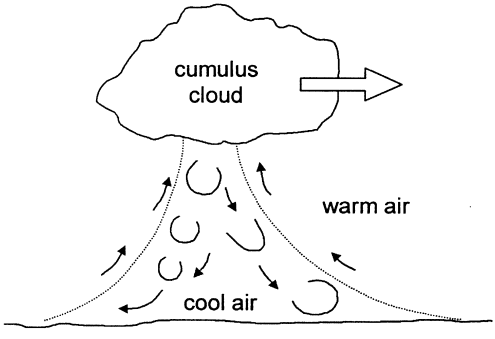

(b)

Figure 1.1 The generation of turbulence in boundary-layer winds and thunderstorm downdrafts.

1.2.2 Coriolis force

The *Coriolis* force is an apparent force due to the rotation of the earth. It acts to the right of the direction of motion in the northern hemisphere, and to the left of the velocity vector, in the case of the southern hemisphere; at the Equator, the Coriolis force is zero. Figure 1.2 gives a simple explanation of the Coriolis force by observing the motion of a particle of air northwards from the South Pole.

Consider a parcel of air moving horizontally away from the South Pole, P, with a velocity U, in the direction of point A (Figure 1.2, left). Since the earth is rotating clockwise with angular velocity, Ω, the point originally at A, will have moved to B, and a point originally at A', will have moved to A, as the air parcel arrives. Relative to the earth's surface, the particle will have appeared to follow the path PA', i.e. to have undergone a continuous deflection to the left. At the North Pole, the deflection is to the right. These deflections can be associated with an apparent acceleration acting at right angles to the velocity of the parcel – the Coriolis acceleration.

Consider a small time interval, δt, (Figure 1.2, right); AA' is then small compared with PA. In this case,

$$AA' = \Omega U(\delta t)^2 \tag{1.2}$$

Let the Coriolis acceleration be denoted by a. Since AA' is the distance travelled under this acceleration, then it can also be expressed by:

$$AA' = (\tfrac{1}{2})a(\delta t)^2 \tag{1.3}$$

Equating the two expressions for AA', equations (1.2) and (1.3),

$$a = 2U\Omega \tag{1.4}$$

This gives the Coriolis acceleration, or force per unit mass, at the poles.

At other points on the earth's surface, the angular velocity is reduced to $\Omega \sin \lambda$, where λ is the latitude. Then the Coriolis acceleration is equal to $2U\ \Omega \sin \lambda$. The term $2\ \Omega \sin \lambda$ is a constant for a given latitude, and is called the 'Coriolis parameter', often denoted by the symbol, f. The Coriolis acceleration is then equal to fU.

Thus, the Coriolis force is an apparent, or effective, force acting to the right of the direction of air motion in the northern hemisphere, and to the left of the air motion in the southern hemisphere. At the Equator, the Coriolis force is zero, and in the Equatorial region, within about 5 degrees of the Equator is negligible in magnitude. The latter explains

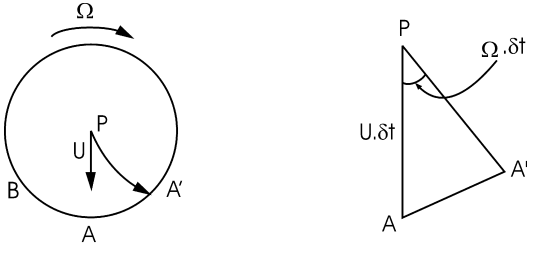

Figure 1.2 The apparent Coriolis force due to the earth's rotation (Southern Hemisphere).

why tropical cyclones (Section 1.3.2), or other cyclonic systems, will not form in the Equatorial regions.

1.2.3 Geostrophic wind

Steady flow under equal and opposite values of the *pressure gradient* and the *Coriolis* force, is called 'balanced geostrophic flow'. Equating the pressure gradient force per unit mass from equation (1.1), and the Coriolis force per unit mass, given by fU, we obtain:

$$U = -\left(\frac{1}{\rho_a f}\right)\frac{\partial p}{\partial x} \tag{1.5}$$

This is the equation for the *geostrophic wind speed*, which is proportional to the magnitude of the pressure gradient, $(\partial p/\partial x)$.

The directions of the pressure gradient and Coriolis forces, and of the flow velocity is shown in Figure 1.3, for both northern and southern hemispheres. It may be seen that the flow direction is parallel to the isobars (lines of constant pressure), in both hemispheres. In the northern hemisphere, the high pressure is to the right of an observer facing the flow direction; in the southern hemisphere, the high pressure is on the left. This results in anti-clockwise rotation of winds around a low-pressure centre in the northern hemisphere, and a clockwise rotation in the southern hemisphere. In both hemispheres, rotation about a low-pressure centre (which usually produces strong winds) is known as a 'cyclone' to meteorologists. Conversely, rotation about a high-pressure centre is known as an 'anti-cyclone'.

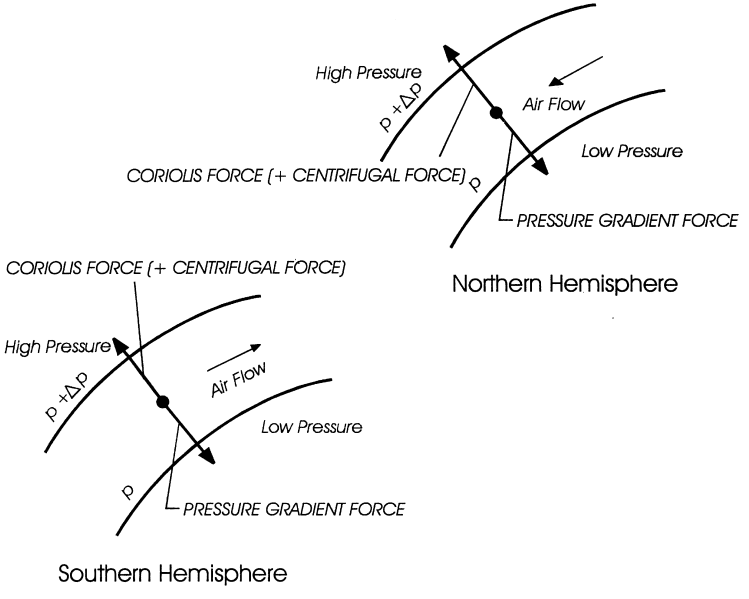

Figure 1.3 Balanced geostrophic flow in the Northern and Southern hemispheres.

1.2.4 Gradient wind

If the isobars have significant curvature (as for example near the centre of a tropical cyclone), then the *centrifugal* force acting on the air particles cannot be neglected. The value of the centrifugal force per unit mass is (U^2/r), where U is the resultant wind velocity, and r is the radius of curvature of the isobars.

The direction of the force is away from the centre of curvature of the isobars. If the path of the air is around a high-pressure centre (anti-cyclone), the centrifugal force acts in the same direction as the pressure gradient force, and in the opposite direction to the Coriolis force. For flow around a low pressure centre (cyclone), the centrifugal force acts in the same direction as the Coriolis force, and opposite to the pressure gradient force.

The equation of motion for a unit mass of air moving at a constant velocity, U, is then equation (1.6) for an anti-cyclone, and (1.7) for a cyclone:

$$\frac{U^2}{r} - |f|U + \frac{1}{\rho_a}\left|\frac{\partial p}{\partial r}\right| = 0 \tag{1.6}$$

$$\frac{U^2}{r} + |f|U - \frac{1}{\rho_a}\left|\frac{\partial p}{\partial r}\right| = 0 \tag{1.7}$$

Equations (1.6) and (1.7) apply to both hemispheres. Note that the pressure gradient $\left|\frac{\partial p}{\partial r}\right|$ is negative in an anti-cyclone and that f is negative in the southern hemisphere. These equations are quadratic equations for the *gradient wind speed*, U. In each case there are two theoretical solutions, but if the pressure gradient is zero, then U must be zero, so that the solutions become:

$$U = \frac{|f|r}{2} - \sqrt{\frac{f^2r^2}{4} - \frac{r}{\rho_a}\left|\frac{\partial p}{\partial r}\right|} \tag{1.8}$$

for an anti-cyclone.

$$U = -\frac{|f|r}{2} + \sqrt{\frac{f^2r^2}{4} + \frac{r}{\rho_a}\left|\frac{\partial p}{\partial r}\right|} \tag{1.9}$$

for a cyclone.

Examining equation (1.8), it can be seen that a maximum value of U occurs when the term under the square root sign is zero. This value is $\frac{|f|r}{2}$, which occurs when $\left|\frac{\partial p}{\partial r}\right|$ is equal to $\frac{\rho_a f^2 r}{4}$. Thus in a anti-cyclone, there is an upper limit to the gradient wind; anti-cyclones are normally associated with low wind speeds.

Now considering equation (1.9), it is clear that the term under the square root sign is always positive. There is therefore no theoretical upper limit to the wind speed in a cyclone; cyclones are therefore associated with strong winds.

1.2.5 Frictional effects

As the earth's surface is approached, *frictional* forces, transmitted through shear between layers of air in the atmospheric boundary layer, gradually play a larger role. This force acts in a direction opposite to that of the flow direction, which in order to achieve a vector balance, is now not parallel to the isobars, but directed towards the low pressure region. Figure 1.4 shows the new balance of forces in the boundary layer. Thus, as the ground surface is approached from above, the wind vector gradually turns towards the low pressure centre, as the height reduces. This effect is known as the *Ekman Spiral*. The total angular change between gradient height and the surface is about 30 degrees. However, the angular change over the height of most tall structures is quite small.

1.3 Types of wind storms

1.3.1 Gales from large depressions

In the mid-latitudes from about 40 to 60 degrees, the strongest winds are gales generated by large and deep depressions or (extra-tropical) cyclones, of synoptic scale. They can also be significant contributors to winds in lower latitudes. Navigators, particularly in sailing ships, are familiar with the strong westerly winds of the 'roaring forties', of which those of the North Atlantic, and at Cape Horn are perhaps the most notorious. As shown in Section 1.4.1, severe building damage has been caused by winter gales in north-west Europe.

These systems are usually large in horizontal dimension – they can extend for more

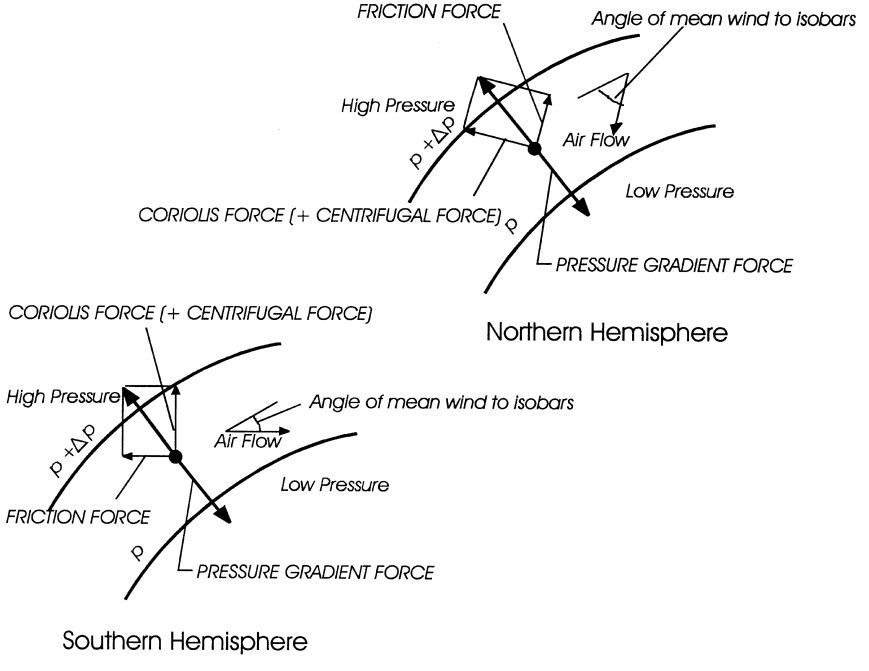

Figure 1.4 Force balance in the atmospheric boundary layer.

than 1,000 kilometres, so can influence large areas of land during their passage – several countries in the case of Europe. They may take several days to pass, although winds may not blow continuously at their maximum intensity during this period. The winds tend to be quite turbulent near the ground, as the flow has adjusted to the frictional effects of the earth's surface over hundreds of kilometres. The direction of the winds remains quite constant over many hours. These features are illustrated in a typical anemograph (wind speed and direction versus time) from this type of event reproduced in Figure 1.5.

1.3.2 Tropical cyclones

Tropical cyclones are intense cyclonic storms which occur over the tropical oceans, mainly in late summer and autumn. They are driven by the latent heat of the oceans, and require a minimum sea temperature of about 26 degrees Celsius to sustain them; they rapidly degenerate when they move over land, or into cooler waters. They will not form within about 5 degrees of the Equator, and do not reach full strength until they reach at least 10 degrees latitude. They are usually at full strength when they are located between 20 and 30 degrees latitude, but can travel to higher latitudes if there are warm ocean currents to sustain them.

The strongest tropical cyclones have occurred in the Caribbean, where they are known as *hurricanes*, in the South China Sea, where they are called *typhoons*, and off the north-west coast of Australia. Areas of medium tropical cyclone activity are the eastern Pacific Ocean off the coast of Mexico, the southern Indian Ocean, the Bay of Bengal, the South Pacific, southern Japan, the Coral Sea (off Eastern Australia) and the south east Atlantic Ocean. Regions of lesser activity or weaker storms are: the Arabian sea, the Gulf of Thailand, and the north coast of Australia (including the Gulf of Carpentaria).

A developed tropical cyclone has a three-dimensional vortex structure which is shown schematically in Figure 1.6. The horizontal dimensions of these storms are less than the extra-tropical cyclones, or depressions, discussed earlier, but their effects can extend for several hundred kilometres. The circulation flows with a radial component towards the 'eye', outside which is a region of intense thermal convection with air currents spiralling upwards. Inside the eye is a region of relative calm with slowly sinking air; the diameter of the eye can range between 8 and 80 km. Often clear skies have been observed in this region. The strongest winds occur just outside the eye wall.

Figure 1.7 gives an example of an anemograph measured at a height of 10 metres above the ground for a tropical cyclone. This example shows a fortuitous situation when the eye of the storm passed nearly directly over the recording station, resulting in a period of about an hour of very low winds. The direction changed nearly 180 degrees during the passage of the vortex over the measuring station.

Outside the eye of a tropical cyclone, the wind speed at upper levels decays with the radial distance from the storm centre. The gradient wind equation (equation (1.9)) can be used to determine this wind speed:

$$U = -\frac{|f|r}{2} + \sqrt{\frac{f^2 r^2}{4} + \frac{r}{\rho_a}\left|\frac{\partial p}{\partial r}\right|} \tag{1.9a}$$

where f is the Coriolis parameter ($=2\,\Omega \sin \lambda$), r is the radius from the storm centre, ρ_a is the density of air and p is the atmospheric pressure.

To apply equation (1.9), it is necessary to establish a suitable function for the pressure gradient. A commonly assumed expression is the following (Holland, 1980):

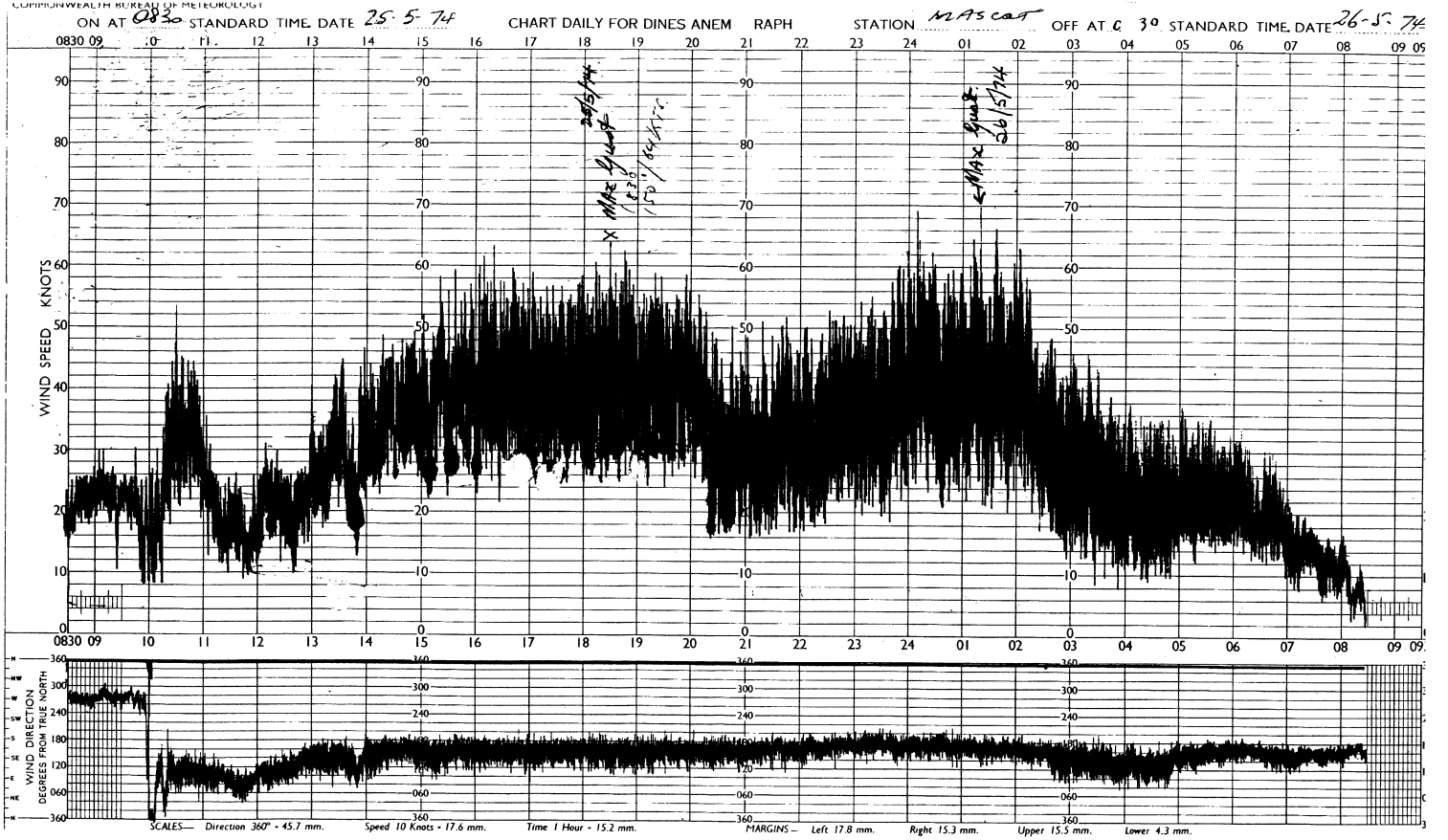

Figure 1.5: Anemograph for synoptic winds from large extra-tropical depression. Time unit: hours.

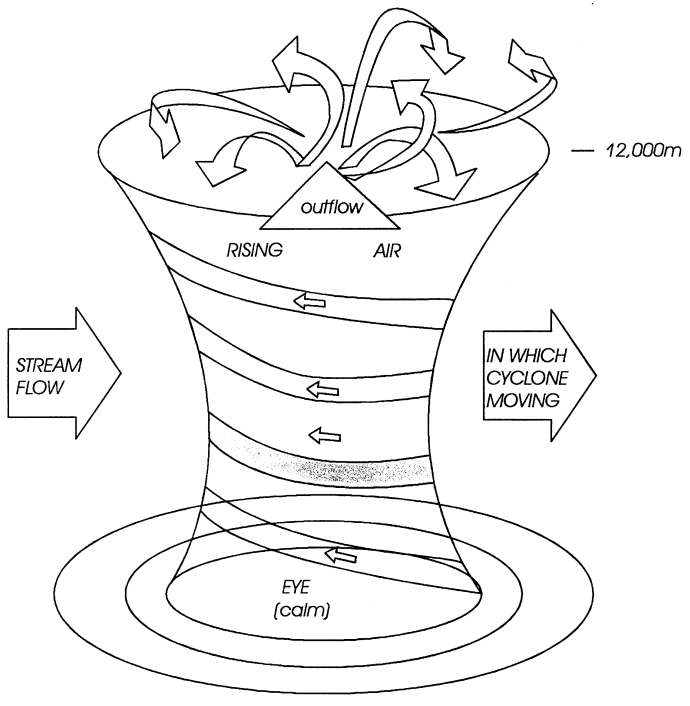

Figure 1.6 Three-dimensional structure in a developed tropical cyclone.

$$\frac{p-p_o}{p_n-p_o} = \exp\left(\frac{-A}{r^B}\right) \tag{1.10}$$

where p_o is the central pressure of the tropical cyclone, p_n is the atmospheric pressure at the edge of the storm and A and B are scaling parameters. The pressure difference (p_n–p_o) can be written as Δp, and is an indication of the strength of the storm.

Differentiating equation (1.10) and substituting in (1.9), we have:

$$U = -\frac{|f|r}{2} + \sqrt{\frac{f^2r^2}{4} + \frac{\Delta p}{\rho_a}\frac{AB}{r^B}\exp\left(-\frac{A}{r^B}\right)} \tag{1.11}$$

This is an equation for the mean wind field at upper levels in a tropical cyclone as a function of radius from the storm centre, r, the characteristic parameters, A and B, the pressure drop across the cyclone, Δp and the Coriolis parameter, f.

Near the centre of a tropical cyclone, the Coriolis forces, i.e. the first two terms in equations (1.9) and (1.11), are small, and it can be shown by differentiating the remaining term that the maximum value of U occurs when r equals $A^{1/B}$. Thus $A^{1/B}$ is to a good approximation, the radius of maximum winds in the cyclone. The exponent B is found to be in the range 1.0 to 2.5, and to reduce with increasing central pressure, p_o, (Holland, 1980).

Figure 1.8 shows the profiles of pressure and gradient wind speed with radial distance from the centre of the storm calculated from equations (1.10) and (1.11), for Cyclone 'Tracy' which severely damaged Darwin, Australia, in 1974. The parameters A and B

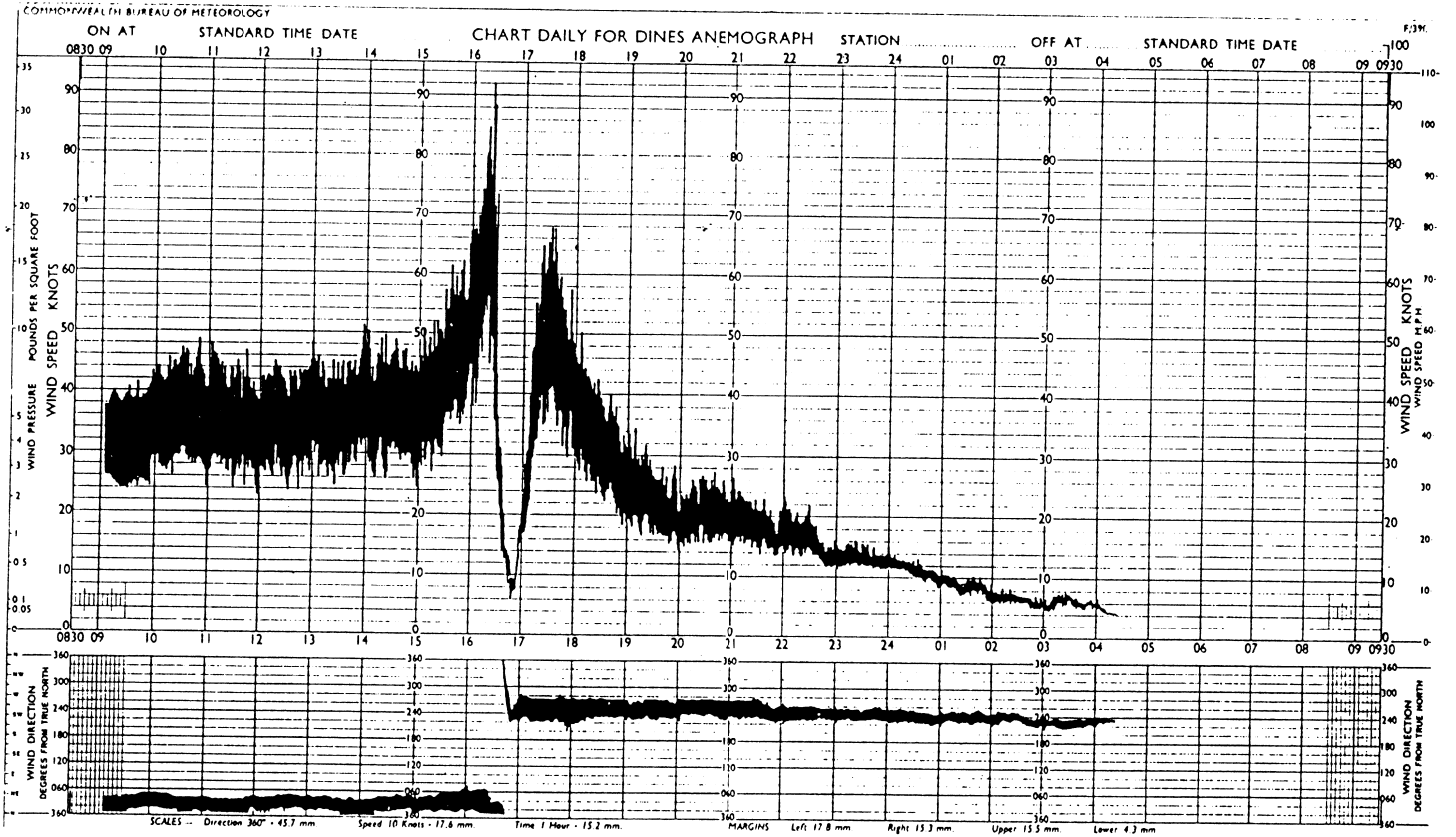

Figure 1.7 Anemograph from a tropical cyclone. Time unit: hours.

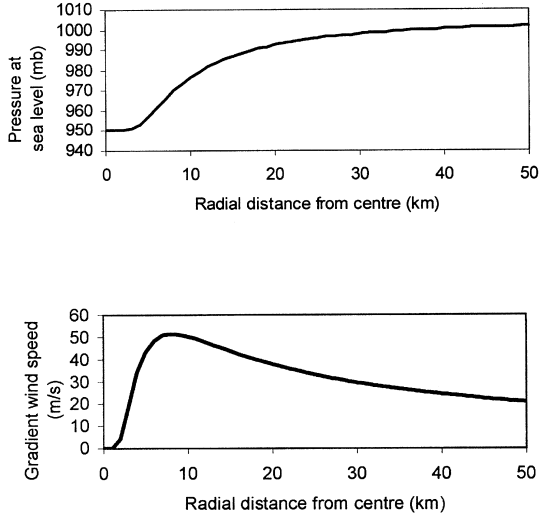

Figure 1.8 Pressure and gradient wind speeds for Cyclone 'Tracy', 1974. (a) Sea level pressure, (b) Gradient wind speed.

were taken as 23 and 1.5, (where r is measured in kilometres), following Holland (1980). The gradient wind speed in Figure 1.8(b), is approximately equal to the gust wind speed near ground level. The radius of maximum winds, in this case about 8 km, approximately coincides with the maximum pressure gradient.

The forward motion of the moving storm adds an additional vector component to the wind speed given by equation (1.11), which gives the wind speed *relative* to the moving storm.

1.3.3 Thunderstorms

Thunderstorms, both isolated storms, and those associated with advancing cold fronts, are small disturbances in horizontal extent, compared with extra-tropical depressions and tropical cyclones, but they are capable of generating severe winds, through tornadoes and downbursts. They contribute significantly to the strongest gusts recorded in many countries, including the United States, Australia and South Africa. They are also the main source of high winds in the Equatorial regions (within about 10 degrees of the Equator), although their strength is not high in these regions.

Thunderstorms also derive their energy from heat. Warm moist air is convected upwards to mix with the drier upper air. With evaporation, rapid cooling occurs and the air mass loses its buoyancy and starts to sink. Condensation then produces heavy rain or hail which falls, dragging cold air with it. A strong downdraft reaches the ground, and produces a strong wind for a short period of time – perhaps 5 to 10 minutes. The strongest winds produced by this mechanism are known as *downbursts*, which are further subdivided into *microbursts* and *macrobursts*, depending on their size. The strongest winds produced by these events have a large component of wind speed due to the forward motion of the convection cell.

The conditions for generation of severe thunderstorms are:

- water vapour in the atmosphere at low levels, i.e. high humidity
- instability in the atmosphere i.e. a negative temperature gradient with height that is greater than the adiabatic rate of the neutral atmosphere
- a lifting mechanism that promotes the initial rapid convection – this may be provided by a mountain range, or a cold front, for example.

1.3.4 Tornadoes

The strongest convection cells, that often generate tornadoes, are known as *supercells*. They are larger and last longer than 'ordinary' convection cells. The tornado, a vertical funnel-shaped vortex created in thunderclouds, is the most destructive of wind storms. Fortunately they are quite small in their horizontal extent – of the order of 100 m – but they can travel for quite long distances up to 50 km before dissipating, producing a long narrow path of destruction. They occur mainly in large continental plains in countries such as the U.S.A., Argentina, Russia and South Africa. Because of their small size they have very rarely passed over a weather recording station.

1.3.5 Downbursts

Figure 1.9 shows an anemograph from a severe thunderstorm downburst, recorded at the Andrews Air Force Base, near Washington, D.C., U.S.A. in 1983, with a time scale in minutes. The short duration of the storm is quite apparent, and there is also a rapid change of wind direction during its passage across the measurement station. Such events typically produce a damage footprint 2–3 km wide and 10–15 km long.

The horizontal wind speed in a thunderstorm downburst with respect to the moving storm is similar to that in a jet of fluid impinging on a plain surface. It varies approximately linearly from the centre of impact to a radius where the wind speed is maximum, and then decays with increasing radius. Again the forward velocity of the moving storm can be a significant component of the total wind speed produced at ground level, and must be added as a vector component to that produced by the jet.

1.3.6 Downslope winds

In certain regions such as those near the Rocky Mountains of the U.S.A., Switzerland, and the Southern Alps of New Zealand, extreme winds can be caused by thermal amplification of synoptic winds on the leeward slopes of mountains. The regions affected are usually quite small, but are often identified as special regions, in wind loading codes and standards (see Appendix D).

1.4 Wind damage

Damage to buildings and other structures by windstorms has been a fact of life for human beings from the time they moved out of cave dwellings to the present day. Trial and error has played an important part in the development of construction techniques and roof shapes for small residential buildings, which have usually suffered the most damage during severe winds. In past centuries, heavy masonry construction, as used for important community buildings such as churches and temples, was seen, by intuition, as the solution to resist wind forces (although somewhat less effective against seismic action). For other types of

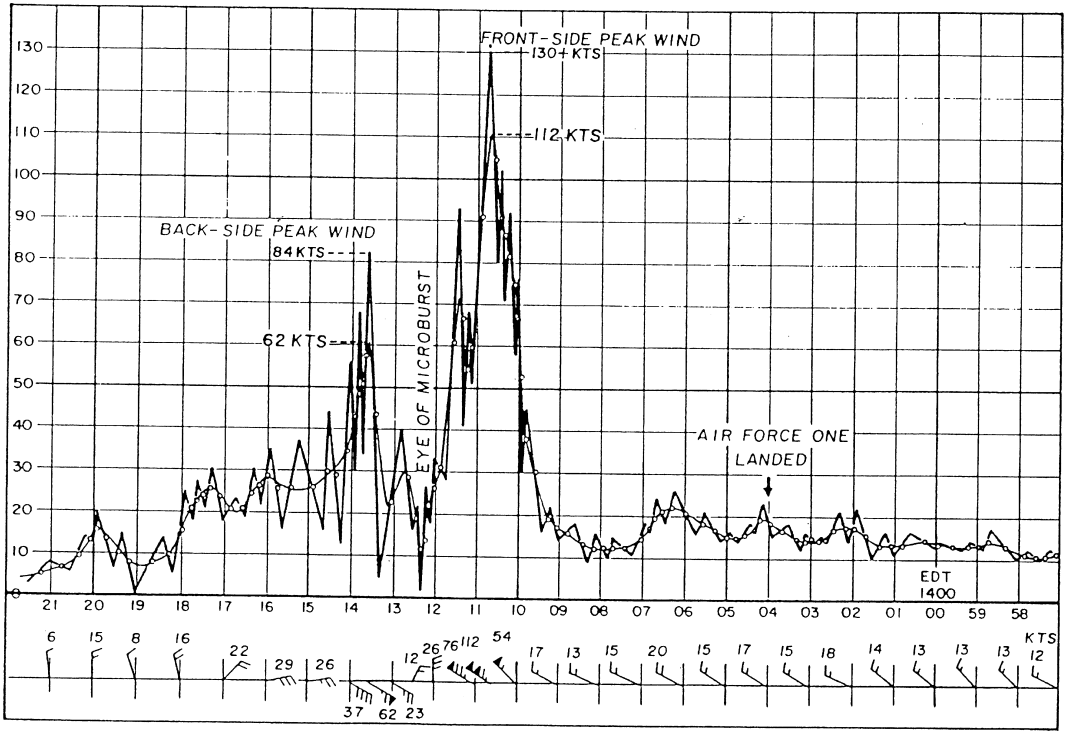

Figure 1.9 Anemograph for a severe downburst at Andrews Air Force Base, Maryland, U.S.A, 1983 (Fujita 1985). Time units: minutes, wind speed: knots.

construction, windstorm damage was generally seen as an 'Act of God', as it is still viewed today by many insurance companies.

The nineteenth century was important as it saw the introduction of steel and reinforced concrete as construction materials, and the beginnings of stress analysis methods for the design of structures. The latter was developed further in the twentieth century, especially in the second half, with the development of computer methods. During the last two centuries, major structural failures due to wind action have occurred periodically, and provoked much interest in wind forces by engineers. Long-span bridges often produced the most spectacular of these failures, with the Brighton Chain Pier, England (1836) (Figure 1.10), the Tay Bridge, Scotland (1879) and Tacoma Narrows Bridge, Washington State, U.S.A. (1940) being among the most notable, with the dynamic action of wind playing a major role.

Other large structures have experienced failures as well – for example, the collapse of the Ferrybridge cooling towers in the U.K. in 1965 (Figure 1.11), and the permanent deformation of the columns of the Great Plains Life Building in Lubbock, Texas, during a tornado (1970). These events were notable, not only as events in themselves, but also for the part they played as a stimulus to the development of research into wind loading in the respective countries. Another type of structure which has proved to be dynamically sensitive to wind, is the guyed mast; it has also suffered a high failure rate – in one 10–year period (from the mid–1980s to the mid–1990s) there were eighty-three failures of this type of structure world-wide. In many cases of mast failures, a combination of wind and ice action was involved.

Some major windstorms, which have caused large scale damage to residential buildings, as well as some engineered structures, are also important for the part they have played in promoting research and understanding of wind loads on structures. The Yorkshire (U.K.) storms of 1962, Cyclone 'Tracy' in Darwin Australia in 1974, and Hurricane 'Andrew' in Florida, U.S.A., in 1992, can be mentioned as seminal events of this type. However, these extreme events occur intermittently, and it is unfortunate that the collective human memory after them is only about 10 years, and often, old lessons have to be relearned by a new generation. However, an encouraging sign is the recent interest of some major insurance and re-insurance groups in natural hazards, in the estimation of the potential financial losses, and the beginnings of a realization that any structure can be made wind-resistant, with appropriate knowledge of the forces involved, and suitable design approaches.

1.4.1 Recent history of wind damage

Figure 1.12 shows the annual insured losses in billions of $US from all major natural disasters, from 1970 to 1999. Windstorms account for about 70% of total insured losses. Bearing in mind that property insurance is much less common in the less-developed economies, Figure 1.12 does not show the total property damage from natural events, and in fact is biased towards losses in Europe and North America. However, the graph does show that the level of insured losses from natural disasters increased dramatically after about 1987. The major contributor to the increase was windstorms, especially tropical cyclones such as Hurricanes 'Hugo' (1989) 'Andrew' (1992) and 'Georges' (1998) in the United States, and winter gales in Europe in 1987, 1990 and 1999.

Some notable windstorms and the losses resulting from them are listed in Table 1.1. Cyclone 'Tracy' and Hurricane 'Andrew' have already been mentioned, but in fact, all

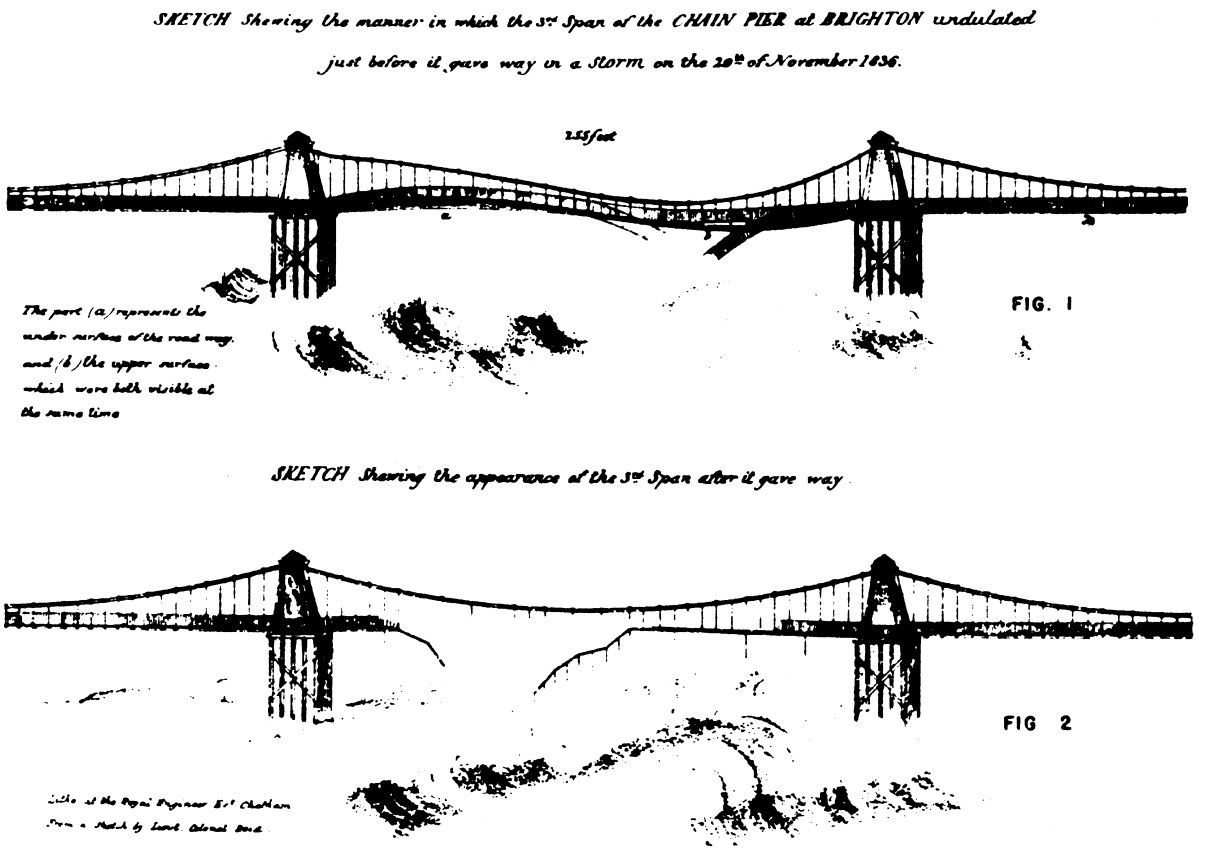

Figure 1.10 Failure of the Brighton Chain Pier, 1836.

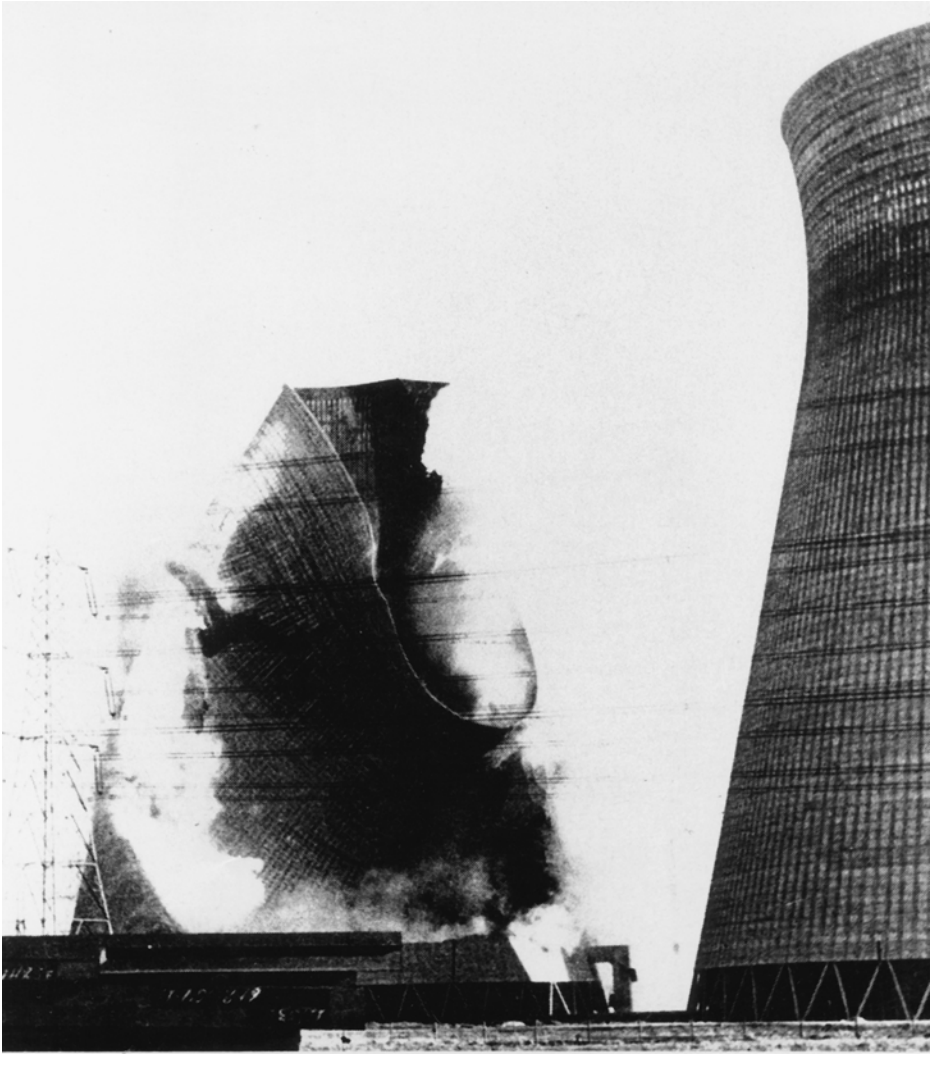

Figure 1.11 Ferrybridge Cooling Tower failures, 1965.

the events listed in Table 1.1 have had a major influences on the insurance industry, and structural engineering profession.

1.5 Wind-generated debris

As well as damage to buildings produced by direct wind forces – either overloads caused by overstressing under peak loads, or fatigue damage under fluctuating loads of a lower level, a major cause of damage in severe wind storms is flying debris. Penetration of the building envelope by flying missiles has a number of undesirable results: high internal pressures threatening the building structure, wind and rain penetration of the inside of the

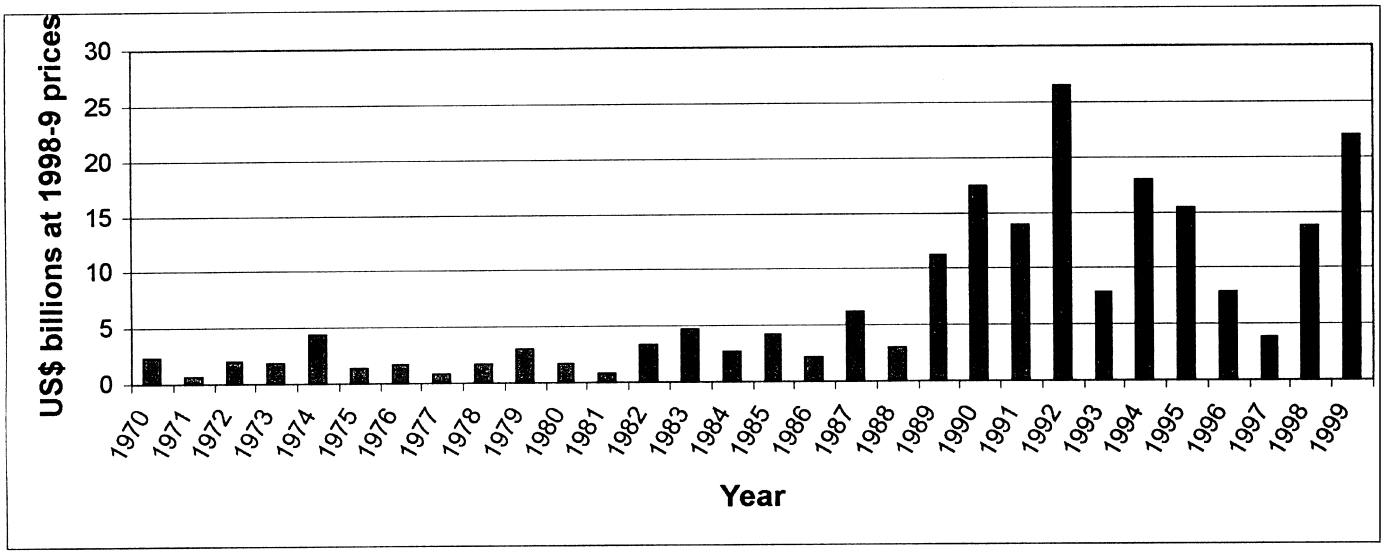

Figure 1.12 World Insurance Losses from Major Natural Disasters (1970–1999). Source: Swiss Reinsurance Company.

Table 1.1 Some disastrous wind storms of the last twenty-five years of the twentieth century

Year	*Name*	*Country or region*	*Economic losses $USmill*	*Lives lost*
1974	Cyclone 'Tracy'	Australia	500	52
1987	Gales	W. Europe	3700	17
1989	Hurricane 'Hugo'	Caribbean, U.S.A.	9000	61
1990	Gales	W. Europe	15000	230
1992	Hurricane 'Andrew'	U.S.A.	30000	44
1999	Gales	France	10000	140

[a] Source of data apart from Cyclone Tracy: Munich Reinsurance.

building, the generation of additional flying debris, and the possibility of flying missiles inside the building endangering the occupants.

The area of a building most vulnerable to impact by missiles is the windward wall region, although impacts could also occur on the roof and side walls. As the air approaches the windward wall, its horizontal velocity reduces rapidly. Heavier objects in the flow with higher inertia will probably continue with their velocity little changed until they impact on the wall. Lighter and smaller objects may lose velocity in this region or even be swept around the building with the flow if they are not directed at the stagnation point (see Chapter 4).

1.5.1 Threshold of flight

Wills *et al.* (1998), carried out an analysis of debris flight conditions, and the resulting building damage in severe winds. They considered 'compact' objects, sheet objects, and rods and poles (Figure 1.13), and established relationships between the body dimensions, and the wind speed, U_f, at which flight occurs and the objects become missiles. For each of the three categories, these relationships are:

$$\ell = \frac{\frac{1}{2}\rho_a U_f^2 C_F}{I\rho_m g} \tag{1.12}$$

$$t = \frac{\frac{1}{2}\rho_a U_f^2 C_F}{I\rho_m g} \tag{1.13}$$

$$d = \frac{\frac{2}{\pi}\rho_a U_f^2 C_F}{I\rho_m g} \tag{1.14}$$

where ℓ is a characteristic dimension for 'compact' objects, t is the thickness of sheet objects, d is the effective diameter of rod-type objects, ρ_a is the density of air, ρ_m is the density of the object material, C_F is an aerodynamic force coefficient (see Section 4.2.2), U_f is the wind speed at which flight occurs, I is a fixing strength integrity parameter, i.e.

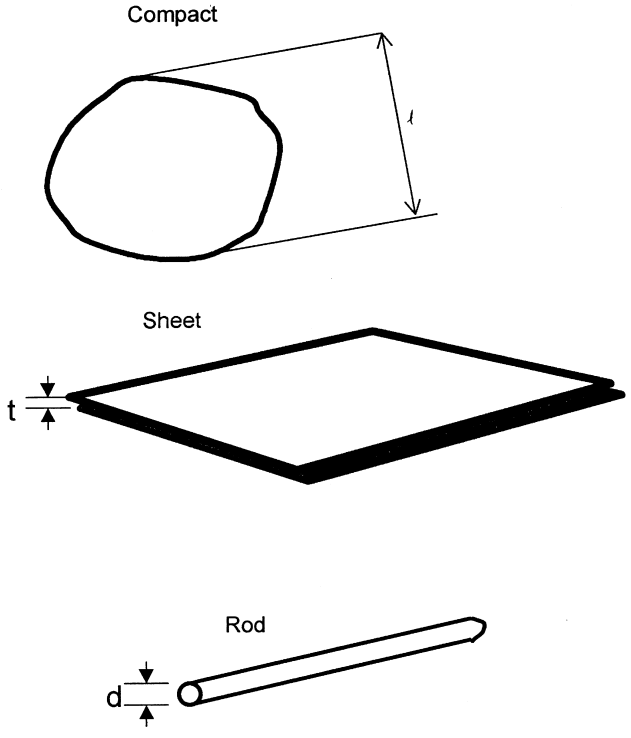

Figure 1.13 Three types of flying debris (after Wills *et al.*, 1998).

the value of force required to dislodge the objects expressed as a multiple of their weight (for objects resting on the ground $I \cong 1$) and g is the gravitational constant.

Equations (1.12), (1.13) and (1.14) illustrate the important point that the larger the value of the characteristic dimension, ℓ, t or d, the higher the wind speed at which flight occurs. These equations also show that the higher the value of the density, ρ_m, the higher is the wind speed for lift off. Thus as the wind speed in a cyclone builds up, the smaller lighter, objects – for example, gravel, small loose objects in gardens and backyards, 'fly' first. At higher wind speeds appurtenances on buildings are dislodged as the wind forces exceed their fixing resistance, and they also commence flight. At even higher wind speeds, substantial pieces of building structure, such as roof sheeting and purlins, may be removed, and become airborne.

As examples of the application of equation (1.12), Wills *et al.* (1998) considered wooden compact objects (ρ_m = 500 kg/m^3) and stone objects (ρ_m = 2700 kg/m^3). Assuming C_F = 1, and I = 1, equation (1.12) gives ℓ equal to 110 mm for the wooden missile, but only 20 mm for the stone missile, for a lift-off speed of 30 m/s.

For sheet objects, equation (1.13) shows that the wind speed for flight depends on the thickness of the sheet, but not on the length and width. Wills *et al.* expressed equation (1.13) in a slightly different form:

$$\rho_m t = \frac{\frac{1}{2}\rho_a U_f^2 C_F}{Ig} \tag{1.13a}$$

The left-hand-side of equation (1.13a) is the mass per unit area of the sheet. This indicates the wind speed for flight for a loose object depends essentially on its mass per unit area. Thus a galvanized iron sheet of 1 mm thickness with mass per unit area of 7.5 kg/m^2 will fly at about 20 m/s (C_F =0.3).

For 'rod'-like objects, which include timber members of rectangular cross-section, a similar formula to equation (1.13a) can be derived from equation (1.14), with the 't' replaced by 'd', the equivalent rod diameter. Using this Wills *et al.* calculated that a timber rod of 10 mm diameter will fly at about 11 m/s, and a 100 mm by 50 mm timber member, with an equivalent diameter of 80 mm, will fly at about 32 m/s, assuming C_F is equal to 1.0.

1.5.2 Flight speeds and accelerations

A missile, once airborne, will continue to accelerate until its flight speed approaches the wind speed, or until its flight is terminated by impact with the ground or with an object such as a building.

The aerodynamic force on a flying object in a wind of speed, U, can be expressed as:

$$\text{Accelerating force} = \frac{1}{2}\rho_a(U-v_m)^2 C_D A$$

where v_m is the velocity of the missile with respect to the ground and A is the reference area for the drag coefficient, C_D (Section 4.2.2).

Applying Newton's law, the instantaneous acceleration of a compact object (characteristic dimension, ℓ) is given by:

$$\text{Acceleration} = \frac{\frac{1}{2}\rho_a(U-v_m)^2 C_D A}{\rho_m \ell^3} = \frac{\frac{1}{2}\rho_a(U-v_m)^2 C_D}{\rho_m \ell} \tag{1.15}$$

taking A equal to ℓ^2.

The same equation applies to 'rod' type objects when ℓ is taken as the length (A is the cross-section area).

Equation (1.15) shows that heavier and larger objects have lower accelerations, and hence their flight speeds are likely to be lower than smaller or lighter objects. The equation also shows that the initial acceleration from rest (v_m = 0) is high, but the acceleration rapidly reduces as the difference between the missile speed and the wind speed reduces, so that the wind speed is approached very slowly. Of course the missile speed cannot exceed the wind speed in steady winds.

Equation (1.15) can be integrated to obtain the time taken to accelerate to a given speed, v_m, and the distance travelled in this time. These equations are as follows:

Time taken to accelerate from 0 to v_m,

$$T = \frac{v_m}{kU(U-v_m)} \tag{1.16}$$

$$\text{Distance travelled,} = U\left[T - \left(\frac{1}{kU}\right)\ln(1 + kUT)\right] \tag{1.17}$$

where $k = (\rho_a C_D)/(2\rho_m \ell)$ with units of (1/m).

Using equation (1.17), the flight times and distance travelled by:

- a steel ball of 8 mm diameter and 2 g mass, and
- a 4 kg piece of timber of 100 mm by 50 mm cross section, and length 1.6 metres,

have been calculated, for a wind speed, U, of 32 m/s, and are given in Table 1.2.

The Table shows the much longer flight times and distances for the larger object. To reach 30 m/s, the timber missile would need to travel for 10 min and over 16 km. In reality, such a long flight time and distance would not occur since the object would strike a building, or the ground, and lose its kinetic energy.

1.5.3 Trajectories of flying debris

Tachikawa (1983) carried out a fundamental study of the trajectories of missiles of the flat plate type. Aerodynamic forces on auto-rotating plates were measured in a wind tunnel. These results were then used to calculate the trajectories of the plates released into a wind stream. Free-flight tests of model plates with various aspect ratios were made in a small wind-tunnel, and compared with the calculated trajectories. A distinct change in the mode of motion and the trajectory, with initial angle of attack of the plate, was observed. The calculated trajectories predicted the upper and lower limits of the observed trajectories, with reasonable accuracy. A later study by Tachikawa (1990) extended the experiments to small prismatic models as well as flat plates, and gave a method of estimating the position of a missile impact on a downstream building. The critical non-dimensional parameter for determination of trajectories was $K = \rho_a U^2 A/2$ mg, where ρ_a is the density of air, U is the wind speed, A is the plan area of a plate, m is the mass of the missile and g is the gravitational constant.

This parameter can also be expressed as the product of three other non-dimensional parameters:

$$K = \frac{1}{2}\frac{\rho_a U^2}{\rho_m g \ell}\frac{\ell}{t} \tag{1.18}$$

where ρ_m is the missile density, t is the plate thickness and ℓ is $\sqrt{A}$, i.e. a characteristic plan dimension.

In equation (1.18), ρ_a/ρ_m is a density ratio and $(U^2/g\ell)$ is a Froude Number, both important non-dimensional quantities in aerodynamics (see also Section 7.4).

Table 1.2 Flight times and distances for two objects

Object/speed	*Time taken (s)*	*Distance travelled (m)*
Steel ball to 20 m/s	5.4	71
Steel ball to 30 m/s	49	1270
Timber piece to 20 m/s	69	910
Timber piece to 30 m/s	625	16300

1.5.4 Damage potential of flying debris

Wills *et al*. (1998) carried out an analysis of the damage potential of flying missiles, based on the assumption that the damage of a given missile is proportional to its kinetic energy in flight. A number of interesting conclusions arose from this work:

- For compact objects, lower density objects have more damage potential
- Sheet and rod objects have generally more damage potential than compact objects
- Very little energy is required to break glass (e.g. 5 g steel ball travelling at 10 m/s is sufficient to break 6 mm annealed glass)
- Based on an assumed distribution of available missile dimensions, Wills *et al*. found that the total damage is proportional to U^n, where n is a power equal to about 5.

1.5.5 Standardized missile testing criteria

In regions subjected to hurricanes and tropical cyclones (Section 1.3.2), where the occurrence of damage to buildings by wind-generated missiles has been shown to be a major problem, standardized missile tests have been devised. These demonstrate the ability of wall claddings of various types to resist penetration by flying debris, or assist in the development of window protection screens.

When specifying appropriate test criteria for missile impact resistance, the following principles should be followed:

- The missiles should be representative of actual objects available
- The criteria should be physically realistic, i.e. if the flight threshold speed is greater than the expected wind speed in the storm, then the object should not be regarded as a potential missile
- Unrealistic flight times and distances should not be implied by the specified missile speed

Missile testing criteria were included in the Darwin Area Building Manual, following Cyclone 'Tracy' in 1974, in Australia. This specified that windows and doors should withstand impact at any angle of a piece of 100 mm by 50 mm timber weighing 4 kg, travelling at 20 m/s. A more severe test was specified for cyclone refuge shelters: 'end-on' impact of a piece of 100 mm by 50 mm timber weighing 8 kg, travelling at 30 m/s. The latter requirement, in particular, was unrealistic, as Table 1.2 demonstrates that it would take several kilometres for such an object to accelerate to 30 m/s. Later the test requirement for windows and doors of buildings was modified to a piece of 100 mm by 50 mm timber weighing 4 kg, travelling at 15 m/s.

Wind-borne debris impact test standards in the United States were discussed by Minor (1994). Following investigations of glass breakage (mainly in high-rise buildings), during several U.S. hurricanes, Pantelides *et al*. (1992) proposed a test protocol involving impacts from small spherical missiles of 2 g. This was taken up in South Florida following Hurricane Andrew in 1992. The Dade County and Broward County editions of the South Florida Building Code require windows, doors and wall coverings to withstand impacts from large and small debris. The large missile test, which is similar to the Australian one, is only applicable to buildings below 9.8 m in height. The small missile test is only applicable to windows, doors and wall coverings above 9.8 m, and differs between the two counties. The Dade County protocol uses ten 2 g pieces of roof gravel impacting simultaneously at

26 m/s, while the Broward County version uses ten 2 g steel balls impacting successively at 43 m/s.

1.6 Insurance loss prediction

The trend towards increased losses from wind storms has provoked concern in the insurance and re-insurance industries, and many of these groups are requiring detailed assessments of the potential financial losses from the exposure of their portfolios of buildings to large-scale severe windstorms. The prediction of average annual loss, or accumulated losses over an extended period, say fifty years, requires two major inputs: hazard models, and vulnerability curves. The hazard model focusses on the wind storm hazard itself, and makes use of historical meteorological data, and statistics to predict potential wind speeds at a site into the future. Vulnerability curves attempt to predict building (and sometimes contents) damage, given the occurrence of a particular wind speed.

1.6.1 Hazard models

The purpose of wind hazard models is to define the risk of occurrence of extreme wind speeds at the site of a single structure, on a system such as a transmission line, or on a complete city or region. The basis for these models is usually the historical record of wind speeds from anemometer stations, but often larger scale storm parameters, such as central pressures for tropical cyclones, and atmospheric stability indices for thunderstorm occurrences, are studied. The methods of statistics and probability are extensively used in the development of hazard models in wind engineering.

The application of statistical methods to the prediction of extreme wind speeds is discussed in Chapter 2 of this book.

An understanding of the structure of the wind within a storm enables predictions of 'footprints' such as that shown in Figure 1.14 (Holmes and Oliver, 2000), which shows simulated contours of maximum wind speeds, occurring at some time during the passage of a downburst (Section 1.3.5). This information, in combination with knowledge of the strength or 'vulnerability' of structures, enables predictions of potential damage to be made.

1.6.2 Vulnerability curves

Insurance loss predictions are quite sensitive to the assumed variations of relative building and contents damage, as a function of the local wind speed. Such graphs are known as

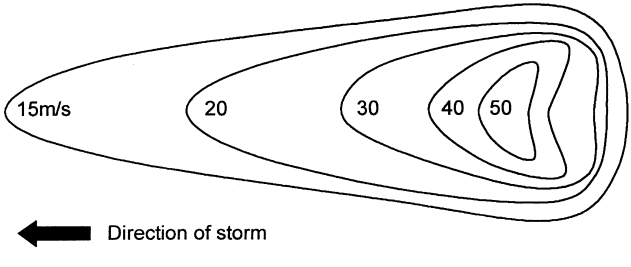

Figure 1.14 Wind speed threshold footprint during the passage of a downburst (Holmes and Oliver, 2000).

'vulnerability curves'. Vulnerability curves can be derived in a number of ways. Leicester (1981) proposed the simplified form, with straight-line segments, for Australian houses, shown in Figure 1.15. The ordinate is a 'damage index' defined as follows for the building:

$$\text{Damage index } (D) = (\text{repair cost})/(\text{initial cost of building})$$

For insurance purposes it may be more appropriate to replace the denominator with the insured value of the building. A similar definition can be applied to the building contents, with 'replacement cost' in the numerator.

Separate lines are given for building and contents. Two parameters only need be specified – a threshold gust speed for the onset of minor damage, and a speed for the onset of major building damage (damage index >0.2).

Walker (1995) proposed the following relationships for housing in Queensland, Australia.

For pre–1980 buildings:

$$D = 0.2\left(\frac{U-30}{30}\right)^2 + 0.5\left(\frac{U-30}{30}\right)^6 \tag{1.19a}$$

For post–1980 buildings:

$$D = 0.2\left(\frac{U-37.5}{37.5}\right)^2 + 0.5\left(\frac{U-37.5}{37.5}\right)^6 \tag{1.19b}$$

Clearly in both cases D is limited to the range 0 to 1.0.

The relationship of equation (1.19a) was also found to agree well with recorded damage and wind speed estimates in Hurricane 'Andrew' (see Table 1.1)

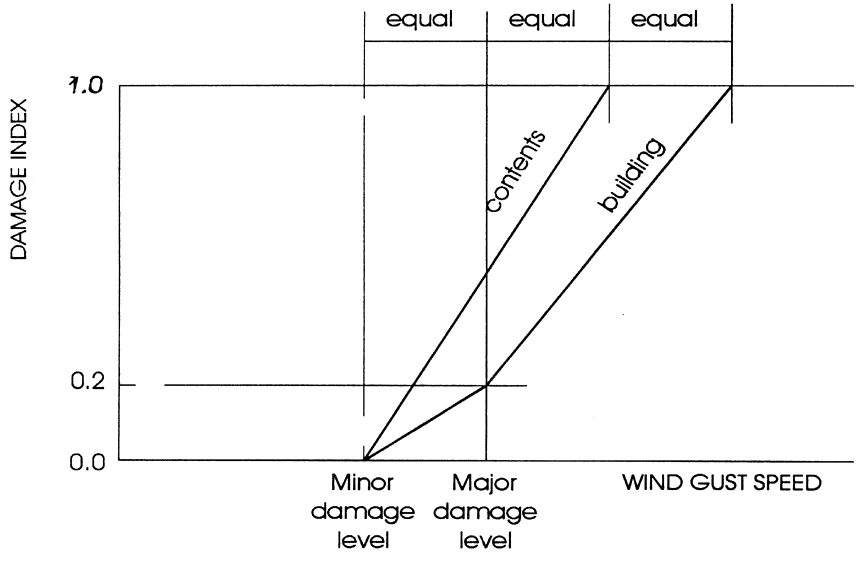

Figure 1.15 Form of vulnerability curve proposed by Leicester (1981).

A simple form of a vulnerability curve for a fully-engineered structure consisting of a large number of members or components with strengths of known probability distribution, can be derived. The failure of each component is assumed to be independent of all the others, and they are all designed to resist the same wind load, or speed. Thus, the expected fractional damage to the complete structure, for a given wind speed, is the proportion of failed components expected at that wind speed. If all the components have the same probability distribution of strength, which would be true if they were all designed to the same codes, then the vulnerability curve can simply be derived from the cumulative distribution of strength of any element.

A curve derived in this way (Holmes, 1996) is shown in Figure 1.16, for a structure comprising of components with a lognormal distribution of strength, with a mean/nominal strength of 1.20, and a coefficient of variation of 0.13, values which are appropriate for steel components. The nominal design gust wind speed is taken as 65 m/s. This curve can be compared with that proposed by Walker, for post–1980 Queensland houses, in the tropical cyclone-affected coastal region (equation 1.19b). The theoretical curve, representing fully-engineered structures, is steeper than the Walker curve which has been derived empirically, and incorporates the greater variability in the components of housing structures.

1.7 Summary

In this chapter, the physical mechanisms and meteorology of strong windstorms of all types, have been described. The balance of forces in a large-scale synoptic system were established, and the gradient wind equation derived. Smaller scale storms – tornadoes and downbursts were also introduced.

The history of significant damaging windstorms was discussed. The mechanics of wind-generated flying debris was considered, and vulnerability curves relating fractional damage potential to wind speed, for insurance loss prediction, were derived.

1.8 The following chapters and appendices

Following this introductory chapter, Chapters 2 to 7 are directed towards fundamental aspects of wind loading, common to all or most structures – for example, atmospheric wind structure and turbulence (Chapter 3), bluff-body aerodynamics (Chapter 4), resonant dynamic response of structures (Chapter 5), and wind-tunnel techniques (Chapter 7). Chap-

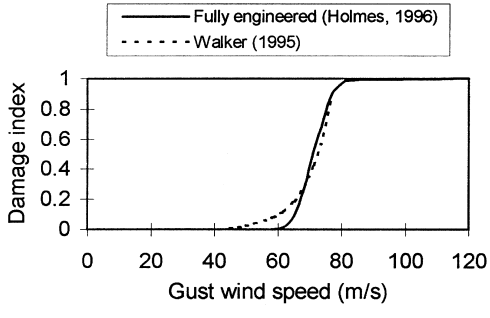

Figure 1.16 Theoretical and empirical vulnerability curves.

ters 8 to 14 deal with aspects of wind loading for particular types of structures: buildings, bridges, towers, etc. Finally, Chapter 15 discusses contemporary wind loading codes and standards – the most common point of contact of practising structural engineers with wind loads.

Appendices A and B cover the terminology of wind engineering and the symbols used in this book, respectively. Appendix C describes probability distributions relevant to wind loading. Appendix D attempts to summarise the extreme wind climate of over fifty countries, and Appendix E gives some approximate formulae for natural frequencies of structures. Appendix F gives a simple example of the calculation of effective static wind load distributions.

References

Fujita, T. T. (1985) *The Downburst. Report on Projects NIMROD and JAWS*. Published by the author at the University of Chicago.

Holland, G. J. (1980) 'An analytic model of the wind and pressure profiles in a hurricane', *Monthly Weather Review* 108: 1212–18.

Holmes, J. D. (1996) 'Vulnerability curves for buildings in tropical-cyclone regions for insurance loss assessment', *ASCE EMD/STD Seventh Specialty Conference on Probabilistic Mechanics and Structural Reliability*, Worcester, Massachusetts, U.S.A., August 7–9.

Holmes, J. D. and Oliver, S. E. (2000) 'An empirical model of a downburst', *Engineering Structures* 22: 1167–72.

Leicester, R. H. (1981) 'A risk model for cyclone damage to dwellings', *Proceedings, 3rd International Conference on Structural Safety and Reliability*, Trondheim, Norway.

Minor, J. E. (1994) 'Windborne debris and the building envelope', *Journal of Wind Engineering and Industrial Aerodynamics* 53: 207–27.

Pantelides, C. P., Horst, A. D. and Minor, J. E. (1992) 'Post-breakage behaviour of architectural glazing in wind storms', *Journal of Wind Engineering and Industrial Aerodynamics* 41–44: 2425–35.

Tachikawa, M. (1983) 'Trajectories of flat plates in uniform flow with application to wind-generated missiles', *Journal of Wind Engineering and Industrial Aerodynamics* 14: 443–53.

—— (1990) 'A method for estimating the distribution range of trajectories of windborne missiles', *Journal of Wind Engineering and Industrial Aerodynamics* 29: 175–84.

Walker, G. R. (1995) *Wind Vulnerability Curves for Queensland Houses*. Alexander Howden Insurance Brokers (Australia) Ltd.

Wills, J., Wyatt, T. and Lee, B. E. (1998) 'Warnings of high winds in densely populated areas', United Kingdom National Coordination Committee for the International Decade for Natural Disaster Reduction.